Environment International 130 (2019) 104885

Contents lists available at ScienceDirect

Environment International

journal homepage: www.elsevier.com/locate/envint

Effects of 2,3,7,8-tetrachlorodibenzo-p-dioxin (TCDD) on the differentiation of embryonic stem cells towards pancreatic lineage and pancreatic beta cell function

John A. Kubi[a,1], Andy C.H. Chen[a,b,1], Sze Wan Fong[a], Keng Po Lai[c], Chris K.C. Wong[d], William S.B. Yeung[a,b], Kai Fai Lee[a,b,*], Yin Lau Lee[a,b,*]

[a] Department of Obstetrics and Gynaecology, The University of Hong Kong, Hong Kong, China
[b] Shenzhen Key Laboratory of Fertility Regulation, The University of Hong Kong Shenzhen Hospital, Shenzhen, China
[c] Department of Chemistry, City University of Hong Kong, Hong Kong, China
[d] Croucher Institute for Environmental Sciences, Department of Biology, Hong Kong Baptist University, Hong Kong, China

ARTICLE INFO

Handling Editor: Hefa Cheng

Keywords:
TCDD
hESCs
Type 2 diabetes (T2D)
PRKAG1
GSIS

ABSTRACT

Animal and epidemiological studies demonstrated association of persistent exposure of TCDD, an endocrine disrupting chemical, to susceptibility of type 2 diabetes (T2D). High doses of TCDD were commonly employed in experimental animals to illustrate its diabetogenic effects. Data linking the epigenetic effects of low doses of TCDD on embryonic cells to T2D susceptibility risks is very limited. To address whether low dose exposure to TCDD would affect pancreatic development, hESCs pretreated with TCDD at concentrations similar to human exposure were differentiated towards pancreatic lineage cells, and their global DNA methylation patterns were determined. Our results showed that TCDD-treated hESCs had impaired pancreatic lineage differentiation potentials and altered global DNA methylation patterns. Four of the hypermethylated genes (*PRKAG1*, *CAPN10*, *HNF-1B* and *MAFA*) were validated by DNA bisulfite sequencing. *PRKAG1*, a regulator in the AMPK signaling pathway critical for insulin secretion, was selected for further functional study in the rat insulinoma cell line, INS-1E cells. TCDD treatment induced *PRKAG1* hypermethylation in hESCs, and the hypermethylation was maintained after pancreatic progenitor cells differentiation. Transient Prkag1 knockdown in the INS-1E cells elevated glucose stimulated insulin secretions (GSIS), possibly through mTOR signaling pathway. The current study suggested that early embryonic exposure to TCDD might alter pancreatogenesis, increasing the risk of T2D.

1. Introduction

Diabetes is a metabolic disease affecting > 400 million people worldwide (American Diabetes, 2014). The major causes of diabetes are pancreas dysfunction and insulin resistance in peripheral cells. Diabetes can be attributed to both genetic and environmental factors (Murea et al., 2012). Among the environmental factors, exposure to synthetic chemicals was shown to increase risks of obesity and T2D (Tang-Peronard et al., 2014). 2,3,7,8-Tetrachlorodibenzo-p-dioxin (TCDD) is one of the endocrine disrupting chemicals (EDCs) well known to destabilize the homeostasis of the body's endocrine system leading to pathologic manifestations such as cardiovascular, reproductive, metabolic, respiratory and neurological disorders (Diamanti-Kandarakis et al., 2009). TCDD is environmental contaminant that accumulates in animal fat. According to the WHO issued review, the mean background levels of TCDD in human tissues range from 2 to 3 parts per trillion (ppt) fat (IARC, 2012), which is equivalent to 6.21–9.31 pM (mean ~ 7 pM). In another report, the toxic equivalencies of TCDD in unexposed human body ranges from 1.86 to 122.99 pM (Consonni et al., 2012). On the other hand, the median serum TCDD concentration in residents near the exposed zone was 173.92 pM (Eskenazi et al., 2004).

In humans, many epidemiological cohort studies have linked persistent TCDD exposure with pathogenesis of T2D (Ngwa et al., 2015; Kern et al., 2004; Cranmer et al., 2000). In a follow-up study on a Vietnam veteran cohort, there was a positive correlation between serum TCDD level and hyperinsulinemia (Cranmer et al., 2000). High level of TCDD exposure is associated with increased serum TCDD level and prevalence of diabetes (Warner et al., 2013). Intriguingly, there was an

* Corresponding authors at: Department of Obstetrics and Gynaecology, Li Ka Shing Faculty of Medicine, The University of Hong Kong, 21 Sassoon Road, Hong Kong, China; Shenzhen Key Laboratory of Fertility Regulation, The University of Hong Kong Shenzhen Hospital, Shenzhen, China.
E-mail addresses: ckflee@hku.hk (K.F. Lee), cherielee@hku.hk (Y.L. Lee).
[1] Co-first authors.

https://doi.org/10.1016/j.envint.2019.05.079
Received 14 February 2019; Received in revised form 21 May 2019; Accepted 31 May 2019
Available online 10 June 2019

inverse correlation between maternal serum TCDD level and birthweight of their offspring in the cohort (Wesselink et al., 2014). The study suggested that TCDD could cross the placental barrier into the intrauterine environment to interfere with fetal development leading to postnatal pathologies (Newbold, 2011; Schug et al., 2011; Ngwa et al., 2015). Growing bodies of in vitro and in vivo animal studies employing persistent exposure of dioxin also strike the relationship between in utero exposure to EDCs and T2D pathogenesis (Ngwa et al., 2015; Alonso-Magdalena et al., 2011; Lee et al., 2014). However, the mechanisms by which TCDD exerts diabetogenic effects remain largely unknown. Epigenetic mechanisms involved in pancreatic lineage development could be a target of TCDD for enhancing the risk of T2D development. Alterations induced by environmental stimuli in DNA methylome of pancreatic islet cells could lead to developmental and functional impairments of the beta cells (Tasnim, 2016; Dayeh and Ling, 2015). A number of human and animal studies correlate aberrant DNA methylation patterns with risks of T2D susceptibility (Tasnim, 2016; Dayeh and Ling, 2015; Dayeh et al., 2013). For example, TCDD dysregulates DNA methylome in pre-implantation embryos (Wu et al., 2004) and immune cells (Winans et al., 2015). However, the relationships between TCDD exposure and DNA methylome during pancreatic development remain unexplored.

We hypothesized in this study that early embryonic exposure to low dose TCDD would alter the DNA methylome and affect early pancreatic lineage development. Embryonic stem cells (ESCs) were utilized as the study model. ESCs are pluripotent cells that can differentiate into different adult cell types (Thomson et al., 1998). In this study, they were used to mimic fetal TCDD exposure. Previous studies using this approach mainly focus on cardiomyocyte differentiation (Neri et al., 2011; Fu et al., 2019). In vitro differentiation of ESCs into pancreatic lineage has been reported to mimic the early pancreas development (Mfopou et al., 2010). Recently, we demonstrated that hyperglycemia impeded differentiation of hESCs to definitive endoderm (DE), an intermediate stage of early pancreatic differentiation (Chen et al., 2017). The current results show that low doses of TCDD exposure dysregulated DNA methylation in hESCs and impaired their differentiation potential to pancreatic lineage cells in vitro. Identification of the etiology of diabetics will help to minimize its risk associated with TCDD exposure or help to develop preventive measures against epigenetic changes in cell differentiation and development.

2. Materials and methods

2.1. Embryonic stem cells (ESCs) culture and TCDD treatments

Human ESC line, VAL3 (Valbuena et al., 2006) was obtained from the Centro de Investigación Príncipe Felipe (CIPF) in Valencia, Spain. The mESCs line (L4) and INS-1E cell line were obtained from the Department of Biochemistry, The University of Hong Kong. VAL3 and L4 were cultured as described (Chen et al., 2017). Briefly, VAL3 cells were seeded at 7.5×10^3 cells/cm^2 on Matrigel coated plates containing mTeSR1 (Stemcell Technologies, Vancouver, Canada). L4 cells were seeded at 1.0×10^4 cells/cm^2 on 0.1% gelatin coated plates containing 2i/LIF medium comprising of DMEM high glucose (Thermo Fisher Scientific, Massachusetts, USA) supplemented with 3 μM CHIR99021 (Tocris, R&D Systems, Minneapolis, USA), 1 μM PD0325901 (Tocris, R&D Systems), 1000 units/ml leukemia inhibitory factor (LIF) (Thermo Fisher Scientific),15% knockout serum replacement (KOSR, Thermo Fisher Scientific), 100 units/ml of penicillin, 100 μg/ml of streptomycin (Thermo Fisher Scientific), 0.1 mM non-essential amino acids (NEAA) (Thermo Fisher Scientific), 2 mM of L-glutamine (L-Glu) (Thermo Fisher Scientific), 1 mM sodium pyruvate (Sigma-Aldrich, Munich, Germany), 0.1 mM β-mercaptoethanol (β-ME) (Sigma-Aldrich), 1× B27 supplement (Thermo Fisher Scientific), 1× N2 supplement (Thermo Fisher Scientific). The ESCs were cultured, maintained and passaged every 3–5 days (Chen et al., 2017). INS-1E cells were cultured and maintained on 0.1% gelatin coated T75 flask (Greiner, Bio-One, Kremsmünster Austria) containing INS-1E cell culture medium RPMI 1640 (Gibco, Thermo Fisher Scientific) supplemented with 50 μM β-ME, 1 mM sodium pyruvate, 10 mM HEPES (sigma Aldrich) and 15% fetal bovine serum (FBS) (Gibco, Thermo Fisher Scientific). The INS-1E cells were passaged every 5–6 days and re-seeded at a ratio of 1:4.

For chronic low doses of TCDD (Sigma-Aldrich) treatments on ESCs, VAL3 and L4 were subjected to TCDD at concentrations of 10 pM or 100 pM in mTeSR1 and 2i/LIF media for two weeks. DMSO (Sigma-Aldrich) was used as the solvent control. The cells were passaged as described above.

2.2. Differentiation of hESCs to pancreatic progenitor cells

VAL3 were differentiated to stage specific pancreatic lineage cells using STEMdiff™ Pancreatic Progenitor Kit (PP kit, Stemcell Technologies) according to the manufacturer's protocol. Briefly, VAL3 at 2.1×10^5 cells/cm^2 were seeded on Matrigel coated plate with mTeSR1 on day 0 (d0). The differentiation was started on d1. Definitive endoderm (DE, stage 1), primitive gut tube (PG, stage 2), posterior foregut (FG, stage 3) and pancreatic progenitor (PP, stage 4) cells were collected on d3, d6, d9 and d15, respectively during the differentiation. The media were changed according to the manufacturer's instruction.

2.3. Differentiation of mESCs to DE cells

L4 cells were induced to DE using a modified protocol (Borowiak et al., 2009). The cells were seeded at 2500 cells/cm^2 on 48 well plates (IWAKI, Japan) containing 2i/LIF medium on d0 and cultured for 2 days. The medium was replaced with serum-free advanced RPMI 1640 medium containing 100 units/ml of penicillin, 100 μg/ml of streptomycin, 2 mM of L-Glu, 5 μM IDE1 (Stemcell Technologies) and the cells were cultured overnight. The cells were then successively cultured in advanced RPMI 1640 medium containing 100 units/ml of penicillin, 100 μg/ml of streptomycin, 2 mM of L-Glu, 0.2% FBS, and 5 μM IDE1 for 2 days, followed by culture in RPMI medium containing the same components with 2% FBS for 5 days. The medium was changed every two days until the end of DE differentiation. The DE cells were collected on d4, d6 and d8 for protocol optimization.

2.4. Quantitative polymerase chain reaction (qPCR) and Western blotting analyses

Total RNAs were extracted by the mirVana PARIS Kit (Thermo Fisher Scientific) and cDNA conversion was performed by the TaqMan Reverse Transcription kit (Thermo Fisher Scientific). Real time qPCR using the TaqMan Gene Expression Assay was performed in an Applied Biosystems 7500 Real-Time PCR System (Applied Biosystems Inc., Thermo Fisher Scientific). Quantifications of *SOX17* (assay ID: Hs00751752_s1; Mm00488363_m1), *FOXA2* (assay ID: Hs05036278_s1; Mm01976556_s1), *POU5F1* (*OCT4*) (assay ID: Hs04260367_gH; Mm03053917_g1), *NANOG* (assay ID: Hs02387400_g1; Mm02019550_s1), *PDX1* (assay ID: Hs00236830_m1; Rn00755591_m1), *SOX9* (assay ID: Hs00165814_m1), *NKX6-1* (assay ID: Hs00232355_m1), *NKX6-2* (assay ID: Hs00752986_s1), *HNF-1B* (assay ID: Hs01001602_m1), *NGN3* (assay ID: Hs01875204_s1), *Eomes* (assay ID: Mm01351984_m1), *Prkag1* (assay ID: Rn01761903_m1), *Ins1* (assay ID: Rn02121433_g1), and *Ins2* (assay ID: Rn01774648_g1) (all from Thermo Fisher Scientific) were determined by the $2^{-\Delta\Delta CT}$ method. Protein level analyses were performed by separating equal amounts of denatured proteins in sodium dodecyl sulfate-polyacrylamide gel electrophoresis (SDS-PAGE) and transferring to polyvinylidene difluoride (PVDF) membrane (Immobilon-P, Millipore). The membranes were incubated successively with primary antibodies against SOX17 and PDX1 (R&D Systems, Minneapolis, USA), AMPKα (D5A2), p-AMPKα (D5A2), AMPKβ1/2 (57C12), PRKAG1, mTOR (7C10), p-mTOR (Ser2448) (Cell

signaling Technology, Massachusetts, USA) and β-actin (Sigma-Aldrich), and appropriate horseradish peroxidase (HRP) conjugated secondary antibodies [Goat anti-mouse IgG, goat anti-rabbit IgG (GE Healthcare, Buckinghamshire, UK), rabbit anti-goat IgG (Santa Cruz Biotechnology, Texas, USA)]. Protein bands were developed in X-ray films using WesternBright ECL Kit (Advansta, California, USA) and were analyzed with ImageJ software.

2.5. Reduced representation bisulfide sequencing and bioinformatics analysis

Total RNase-free genomic DNA was extracted by the DNeasy blood and tissue kit (Qiagen, Maryland, USA) according the manufacturer's instruction. DNAs (2.5 μg) isolated from DMSO or TCDD treated VAL3 cells were sent to the Center for Genomic Sciences (HKU) for reduced representation bisulfide sequencing (RRBS). For the library construction and subsequent sequencing procedures, the genomic DNA was subjected to an overnight restriction enzyme *MspI* (BioLabs, New England, USA) digestion. The QIAquick Nucleotide Removal Kit (Qiagen) was employed to purify the digested DNA. The KAPA Hyper Prep Kit (KAPABiosystems, Massachusetts, USA) was used to introduce an extra adenosine (A) at the 3′ terminal of plus and minus strands of the purified DNA during end-repair and A-tailing process to facilitate downstream adaptor ligation. The methylated indexed adapter (120 bp) was then ligated at the terminal ends using SeqCap Adapter Kits (Roche Life Science, California, USA). The constructed libraries were purified using the AMPure beads (Beckman Coulter, Florida, USA) and the library sizes ranging from 150 bp to 350 bp were excised by the BluePippin with 3% agarose gel cassette (Marker Q2) (Sage Science, Massachusetts, USA). Size-selected libraries were subjected to bisulfite conversion using the EZ DNA Methylation-Lightning Kit (Zymo Research, California, USA). The bisulfite converted libraries were subjected to 12 cycles of amplification with the PfuTurbo Cx Hotstart DNA Polymerase (Agilent Technologies, California, USA) and Library Amplification Primer Mix (KAPABiosystems). The qualities and quantities of the amplified libraries were evaluated using a 2100 Bioanalyzer high sensitivity DNA assay (Agilent Technologies) and the Qubit dsDNA high sensitivity assay (Life Technologies, California, USA) respectively. The libraries were denatured, diluted to optimal concentration and applied in the cluster generation steps using the HiSeq PE Cluster Kit v4 with cbot (Illumina, San Diego, USA). The Illumina HiSeq SBS Kit v4 (Illumina) was used for paired-end 101 bp sequencing. Sequence reads were trimmed by the Trimgalore, which was optimized for RRBS data. The reads were then mapped by whole genome Bisulfite Sequence MAPping program (BS-MAP) onto hg38, followed by model based analysis of bisulfite sequencing data (MOABS) (Sun et al., 2014). The results show methylation differences in each CpG site between TCDD treatment group and DMSO control group. Methylation differences $>$ 0.2 were considered significant for further analysis. The TCDD induced differentially methylated genes generated from the methylome data were subjected to Gene Ontology (GO) and Kyoto Encyclopedia of Genes and Genomes (KEGG) analyses using online Database for Annotation, Visualization and Integrated Discovery (DAVID 6.8) analysis tool (Huang da et al., 2009).

2.6. Bisulfite sequencing

Primers were designed for amplifying the differentially methylated regions of the selected targets (Supplementary Table 1). The extracted DNAs were subjected to bisulfite conversion using the Epitect Bisulfite Kit Protocol (Qiagen). The bisulfite converted DNA was mixed with 25 μl of Hot start Taq 2× master mix (BioLabs, New England) and predesigned primers of the target genes *PRKAG1*, *CAPN10*, *HNF-1B*, and *MAFA*. The targeted regions of the selected genes were amplified, and the PCR products were purified using the GeneJet PCR Purification kit (Thermo Fisher Scientific) and ligated into a vector using the pGEM®-T Easy Vector System (Promega, Southampton, United Kingdom). The ligation reaction mixtures were mixed with the DH5α competent cells (Thermo Fisher Scientific) and spread on LB/ampicillin/IPTG/X-Gal plates for overnight incubation at 37 °C and 5% CO_2. The plasmid DNAs were extracted and purified using the QIAprep spin miniprep kit (Qiagen) and sent out for DNA sequencing (Tech Dragon Ltd, Hong Kong).

2.7. siRNA transfection

INS-1E cells were transfected with 125 nM, 250 nM or 500 nM Prkag1 or scramble control siRNA (Thermo Fisher Scientific) using lipofectamine 2000 (Thermo Fisher Scientific). Seventy-two hours after transfection, the cells were starved for 3 h in glucose free Krebs-Ringer-HEPES buffer (KRHB) (Marshall et al., 2005) followed by 30 minute basal (2.5 mM) and stimulatory (15 mM) glucose treatments in KRHB. The glucose stimulated insulin secretions (GSIS) in the conditioned media were measured using the human insulin ELISA kit (Abcam, Massachusetts, USA) and the cell pellets were processed for qPCR and western blot analysis.

2.8. Statistical analysis

Gene and protein expressions were subjected to statistical assessments using Graphpad (Prism 5) or SigmaPlot 12.0 software. The generated data were statistically analyzed by employing one-way analysis of variance (ANOVA), Mann Whitney Rank Sum test or Chi-square test where appropriate. The data in the plots were represented as the mean ± standard error of mean (SEM). A P-value $<$ 0.05 was considered as statistical significance.

3. Results

3.1. TCDD treatment impaired hESCs and mESCs differentiation potentials towards pancreatic lineage

Human ESCs were subjected to DE, PG, FG, and PP differentiation using the PP kit. The results showed that the pluripotent marker *OCT4* was significantly reduced whereas markers of DE (*SOX17*, *FOXA2*), FG (*HNF-1B*) and PP (*PDX1*, *SOX9*, *NKX6-1*, *NKX6-2* and *NGN3*) were upregulated upon differentiation (Supplementary Fig. S1). Mouse ESCs (L4) was also induced to DE. Similarly, pluripotent markers (*Oct4* and *Nanog*) were significantly suppressed while DE markers (*Sox17* and *Foxa2*) were significantly upregulated after DE differentiation. The mRNA level of mesendoderm marker, *Eomes* was upregulated only on day 4 of DE differentiation (Supplementary Fig. S2). We then cultured hESCs with low doses of TCDD (10 pM and 100 pM) or the solvent control, DMSO for two weeks and subsequently differentiated the hESCs towards pancreatic lineage using the PP kit. The results revealed that the *OCT4* mRNA levels were significantly lower in both the 10 pM and 100 pM TCDD-treated hESCs when compared to the control prior to differentiation ($P < 0.05$, Fig. 1A). On the contrary, *OCT4* mRNA levels were found to be significantly higher in the TCDD (10 pM and 100 pM) treated-hESCs-derived DE when compared to the corresponding DMSO control ($P < 0.05$, Fig. 1A). However, such phenomenon was not observed in another pluripotent gene, *NANOG* (Fig. 1B). When the cells were differentiated into FG and PP stages, both *OCT4* and *NANOG* were significantly down-regulated (Fig. 1A and B). Interestingly, high levels of *SOX17* were detected at the DE stage only. *SOX17* mRNA levels was significantly lower in the TCDD-treated groups as compared to the DMSO control (Fig. 1C). The levels of *FOXA2* increased progressively from the DE to the PP stage. However, *FOXA2* levels in the TCDD-treated groups were not efficiently induced at these stages, and no statistical significance was found among groups (Fig. 1D). Furthermore, 10 pM but not 100 pM TCDD significantly suppressed *PDX1* expression at the PP stage as compared to that of the

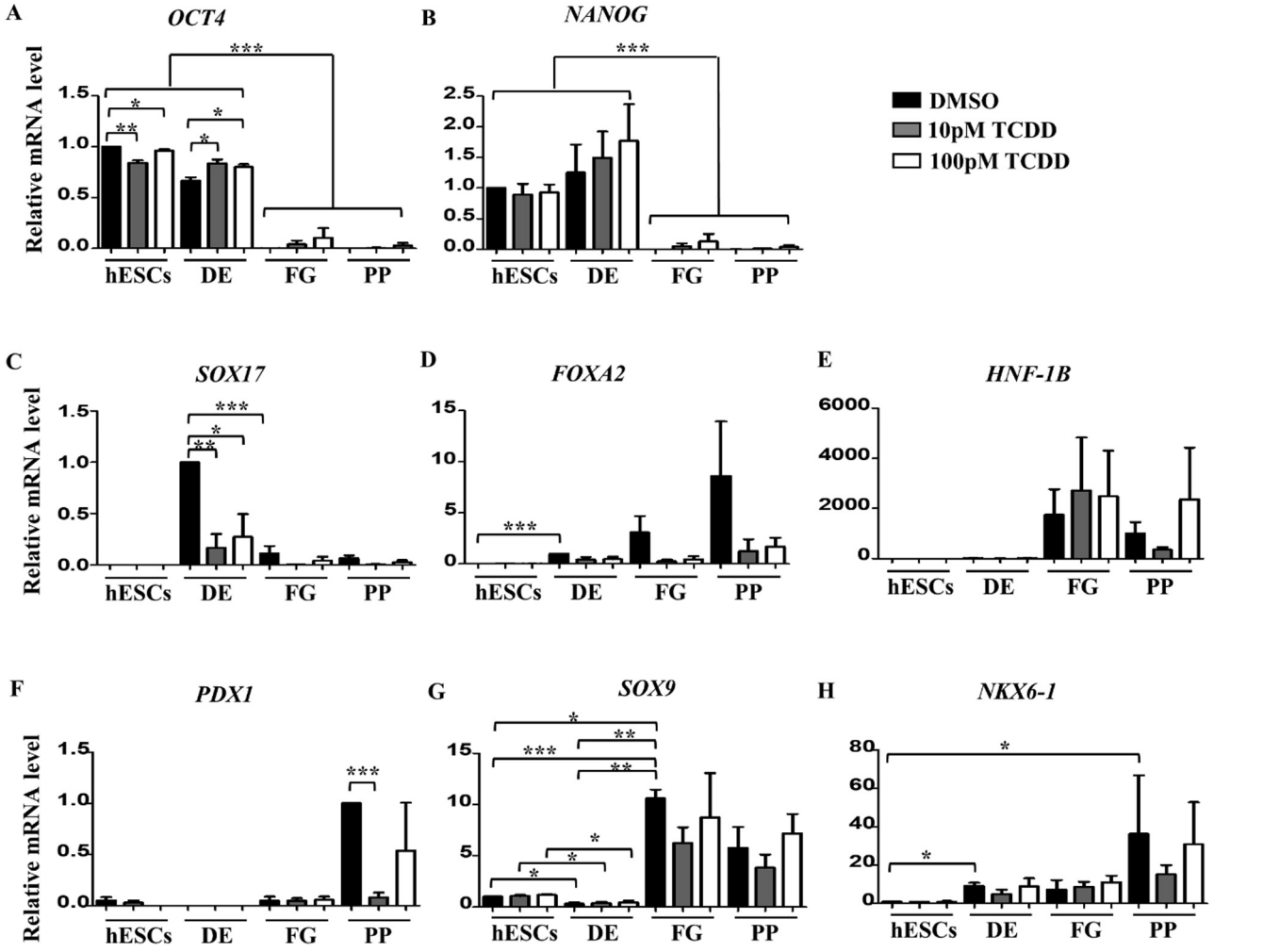

Fig. 1. Expression patterns of key marker genes during PP differentiation of TCDD-treated VAL3 hESCs. TCDD or DMSO treated VAL3 were differentiated into DE, FG and PP stages. The mRNA levels of (A) *OCT4*, (B) *NANOG*, (C) *SOX17*, (D) *FOXA2*, (E) *HNF-1B*, (F) *PDX1*, (G) *SOX9*, and (H) *NKX6-1* were analyzed by qPCR. Expression was normalized to 18S ribosomal RNA. The DMSO group of the DE stages was set as calibrators for *SOX17* and *FOXA2*, the DMSO group of the PP stage was used as the calibrator for *PDX1* and the remaining stage specific gene expressions were relative to the DMSO groups of hESCs. *: $P < 0.05$, **: $P < 0.01$, ***: $P < 0.001$; Mann Whitney Rank Sum Test; n = 3.

DMSO ($P < 0.001$, Fig. 1F). TCDD treatments however had no significant effects on the FG marker, *HNF-1B* (Fig. 1E), and other PP markers, *SOX9* (Fig. 1G) and *NKX6-1* (Fig. 1H).

Mouse ESCs, L4 cells were also subjected to low doses of TCDD or DMSO treatments for five passages followed by differentiation into DE. TCDD treatments significantly repressed *Oct4* mRNA levels in undifferentiated mESCs (Fig. 2A). *Sox17* mRNA levels were significantly lowered at the DE stages in both the 10 pM and the 100 pM TCDD-treated cells as compared to the DMSO control ($P < 0.05$, Fig. 2B). Additionally, the 100 pM TCDD treated L4 also had significantly lower *Foxa2* mRNA levels as compared to DMSO group (Fig. 2C).

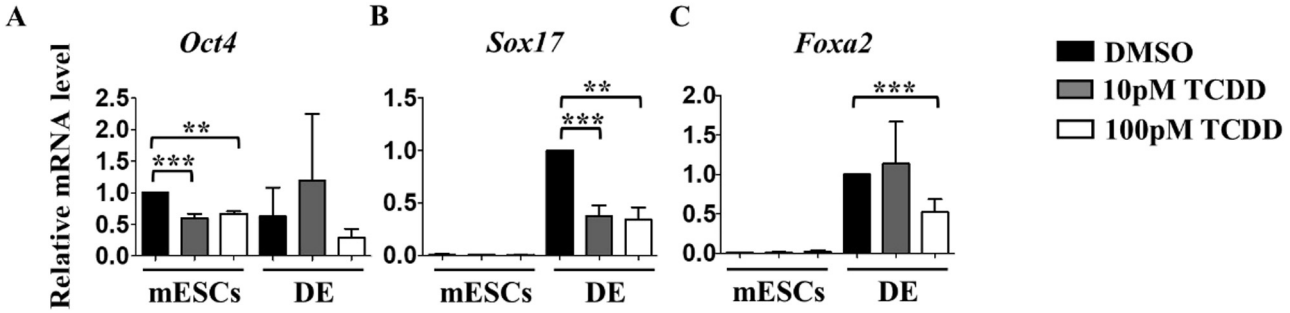

Fig. 2. Expression patterns of DE genes during DE differentiation of TCDD treated L4 mESCs. TCDD or DMSO treated mESCs were differentiated into DE. The gene expressions of (A) *Oct4*, (B) *Sox17* and (C) *Foxa2* were analyzed by qPCR. Expression was normalized with 18S ribosomal RNA. The mRNA levels were relative to DMSO group of mESCs. **: $P < 0.01$, ***: $P < 0.001$; one-way ANOVA and Mann Whitney Rank Sum Test; n = 4.

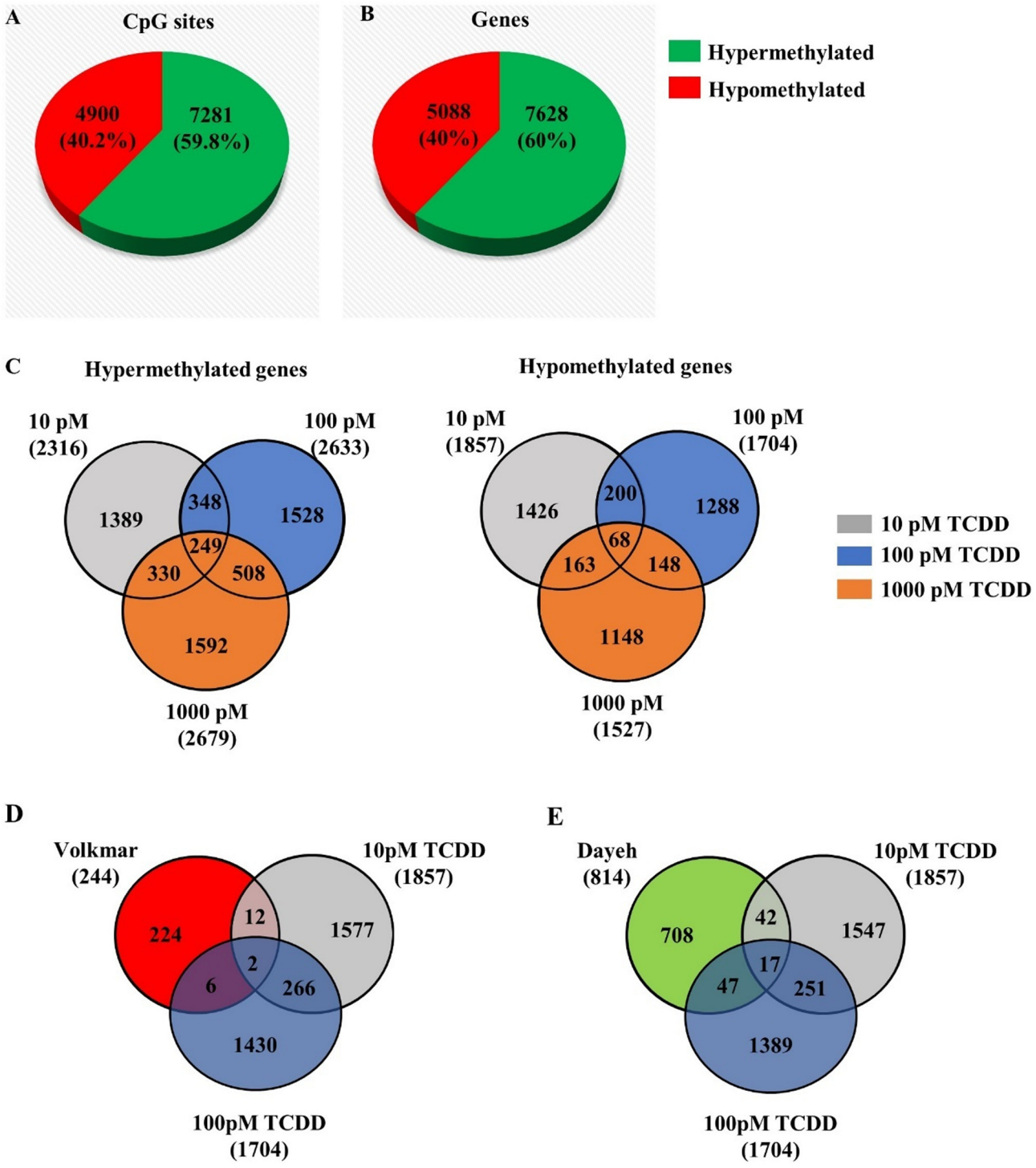

Fig. 3. DNA methylation changes induced by TCDD treatments in hESCs.
(A, B) Distribution of differentially hypomethylated and hypermethylated CpG sites and corresponding genes upon TCDD treatments. (C) Venn diagram illustrating the number of common genes hyper- or hypomethylated by different doses of TCDD treatments. (D, E) Number of common genes differentially hypomethylated in TCDD-treated hESCs and T2D patients reported in Volkmar's (D) and Dayeh's (E) studies.

3.2. TCDD treatments induced global DNA methylation changes in non-differentiated hESCs

To study the effects of TCDD treatments on global DNA methylation changes in hESCs, we treated hESCs with low (10 pM and 100 pM) and high dose (1000 pM) of TCDD for two weeks. The extracted DNA was subjected to reduced representation bisulfite sequencing (RRBS) for generating the methylome data. Bioinformatics analysis of the data revealed that the TCDD treatments induced a total of 12,181 differentially methylated CpG (5′-cytosine-phosphate-guanine-3′) sites in the undifferentiated hESCs, in which 7281 were hypermethylated and 4900 were hypomethylated (Fig. 3A). The TCDD induced differentially methylated CpG sites corresponded with 7628 hypermethylated genes and 5088 hypomethylated genes (Fig. 3B). The low and high doses of TCDD induced similar number of hypermethylated (10 pM: 2173, 100 pM: 2539, 1000 pM: 2569) and hypomethylated (10 pM: 1783, 100 pM:

1639, 1000 pM: 1478) CpG sites, corresponding to 2316, 2633, 2679 hypermethylated, and 1857, 1704, 1527 hypomethylated genes in the 10 pM, 100 pM and 1000 pM TCDD treated cells, respectively. The corresponding genes were subjected to Venn diagram analysis and the data showed there were 249 hypermethylated and 68 hypomethylated genes commonly induced by the three doses of TCDD treatments (Fig. 3C). While the low doses of TCDD commonly induced 597 hypermethylated genes and 268 hypomethylated genes in the hESCs, 1592 hypermethylated genes and 1148 hypomethylated genes were exclusively induced at high dose (Fig. 3C).

We then compared the low doses induced differentially methylated genes with the reported differentially methylated genes in T2D patients' pancreatic islets (Dayeh et al., 2014; Volkmar et al., 2012). Out of 244 hypomethylated genes reported in the Volkmar's group, 12 and 6 unique hypomethylated genes were found in the 10 pM and the 100 pM TCDD treatments, respectively. Two hypomethylated genes (*TMC8*, *SLC25A5*) were found in the Volkmar's study, 10 pM and 100 pM TCDD groups (Fig. 3D). None of the 10 hypermethylated genes found in Volkmar's study matched with any of the TCDD induced hypermethylated genes. Out of the 814 hypomethylated genes found by the Dayeh's group, 42 and 47 unique hypomethylated genes were found in the 10 pM and the 100 pM TCDD treated hESCs (Fig. 3E). There are 17 common hypomethylated genes found in the Dayeh's study, 10 pM and 100 pM TCDD treatment groups. Furthermore, 3 hypermethylated genes (*SEMA4A*, *NBEAL2* and *CACNA1H*) were commonly found in the Dayeh's study and the 10 pM and/or 100 pM TCDD induced hypermethylated gene list (Supplementary Table 2).

3.3. Gene ontology analysis of low doses of TCDD induced methylated genes

The 597 hypermethylated and 268 hypomethylated genes found common to the low doses of TCDD treatments (Fig. 3C) were subjected to gene ontology analysis using DAVID Bioinformatics Resources 6.8 (Fig. 4A–B). The hypermethylated genes resulted in only 13 enriched GO terms of biological processes and one KEGG pathway. Among them, positive regulation of protein kinase activity was the most significantly enriched GO term ($P < 0.001$, Fig. 4A). For the hypomethylated gene list, only 3 GO terms were significantly enriched ($P < 0.05$, Fig. 4B). The 1000 pM TCDD induced differentially methylated genes were enriched in diverse biological processes and functions such as embryonic camera-type eye morphogenesis, skin development, response to hypoxia, intracellular protein transport, etc. (Supplementary Fig. S3A–B). We then focused on the low doses of TCDD enriched GO terms and KEGG pathways that are related to pancreatic lineage cells development and functions. Genes related to insulin signaling pathway, notch signaling pathways and Type II diabetes mellitus were significantly enriched in the 10 pM TCDD induced hypermethylated group (red, Fig. 4C). On the other hand, KEGG pathways related to cardiomyocytes were enriched in the 100 pM TCDD induced hypermethylated group (blue, Fig. 4D).

We further analyzed the distances in base pairs (bp) of low doses of TCDD induced differentially methylated CpG sites (DMCS) proximal (0–2 kbp) and distal (> 2 kbp) to the transcription start sites (TSS). It was found that 10 pM TCDD treatment induced 1509 hypermethylated and 1608 hypomethylated gene regions near the TSS, while 100 pM TCDD treatment induced 1177 hypermethylated and 1107 hypomethylated gene regions near the TSS (Fig. 5A). The numbers of differentially methylated CpG sites across chromosomes were similar between different TCDD doses. The numbers of differentially methylated CpG sites were also associated with the numbers of protein coding genes across different chromosomes in hESCs (Yan et al., 2013) (Supplementary Fig. S4). GO term and KEGG pathway analysis showed that the TCDD induced differentially methylated gene regions near the TSS were significantly enriched in pancreatic development and functions as well as cardiomyocyte development ($P < 0.05$, Fig. 5B–C).

3.4. Validation of selected hypermethylated genes by DNA bisulfite sequencing

We selected the pancreatic lineage differentiation and/or functions related genes *PRKAG1*, *CAPN10*, *HNF-1B* and *MAFA* (Supplementary Tables 2–5) for validation of the methylation status after TCDD treatments. Targeted regions (in grey, Fig. 6) of bisulfite converted DNA from the TCDD (10 or 100 pM) or DMSO treated hESCs were amplified with the primers followed by DNA sequencing. The sequencing results showed that the 100 pM but not the 10 pM TCDD significantly induced DNA hypermethylation at only one site near the promoter regions of *PRKAG1* (CpG site −689, Fig. 6A), *CAPN10* (CpG site −741, Fig. 6B) and *HNF-1B* (CpG site +991, Fig. 6C), and two sites of *MAFA* (CpG sites +473 and +516, Fig. 6D) in the hESCs state.

3.5. TCDD induced PRKAG1 hypermethylation at the hESCs state was maintained after differentiated into PP stage

TCDD (10 pM or 100 pM) or DMSO treated hESCs were subjected to PP kit differentiation. The *PRKAG1* targeted region of bisulfite converted DNA from the differentiated cells was followed (Fig. 7A). The results revealed that the validated 100 pM induced hypermethylated CpG site −689 (Fig. 6A) was still maintained in the TCDD-treated hESCs-derived PP stage (Fig. 7B). Interestingly, the methylation of another CpG site, −579 was not statistically different in the TCDD treatment groups at the undifferentiated hESCs state but became significantly hypermethylated at PP stage after 100 pM TCDD treatment (Fig. 7B). A trend of induced hypermethylation post-10 pM TCDD treatment on the CpG sites −689 and −579 (Fig. 6A) at the undifferentiated hESCs was maintained at the PP stage (Fig. 7B), though the differences were not statistically significant.

3.6. Prkag1 knockdown reduced AMPK protein expressions, activated mTOR1 pathway and increased glucose stimulated insulin secretion (GSIS) in INS-1E cells

Prior to the Prkag1 functional studies, we confirmed the responsiveness of INS-1E cells to glucose challenges and optimized the dilution factors of the INS-1E cells conditioned medium (CM) for insulin secretory measurement within the detection limit of the insulin ELISA kit. We then optimized the knockdown efficiency of Prkag1 by siRNA transfection in INS-1E with different concentrations of scrambled or Prkag1 siRNA (125 nM, 250 nM and 500 nM). All the three concentrations of Prkag1 siRNA significantly suppressed *Prkag1* mRNA levels in the transfected cells when compared with their scrambled controls (Supplementary Fig. S5A, $P < 0.05$). The 250 nM and 500 nM but not 125 nM Prkag1 siRNA significantly reduced the Prkag1 protein levels in the transfected cells when compared with their corresponding scrambled siRNA controls (Supplementary Fig. S5B, $P < 0.05$). qPCR result showed that Prkag1 knockdown had no effect on *ins1*, *ins2* and *pdx1* mRNA levels (Supplementary Fig. S5B).

To investigate the Prkag1 knockdown effects on the responsiveness of INS-1E cells to glucose challenge, the Prkag1 and scrambled siRNA transfected INS-1E cells were starved for 3 h and subsequently subjected to 30 min of basal and stimulatory glucose treatments. As expected, the protein levels of Prkag1 were all down regulated in both 250 nM and 500 nM Prkag1 siRNA treated cells (Fig. 8A). In these cells, significantly lower protein levels of AMPKα and AMPKβ2, but not AMPK β1 were detected when compared with that of the scrambled siRNA control groups ($P < 0.05$, Fig. 8B and C). Western blotting results also showed that the 500 nM Prkag1 siRNA significantly elevated the ratio of phosphorylated mTOR to the total mTOR protein levels in the transfected cells when compared with the corresponding scrambled siRNA control in glucose stimulatory conditions (Fig. 8D). The ELISA results revealed that Prkag1 siRNA significantly increased GSIS in the transfected cells when compared with the scrambled control ($P < 0.05$,

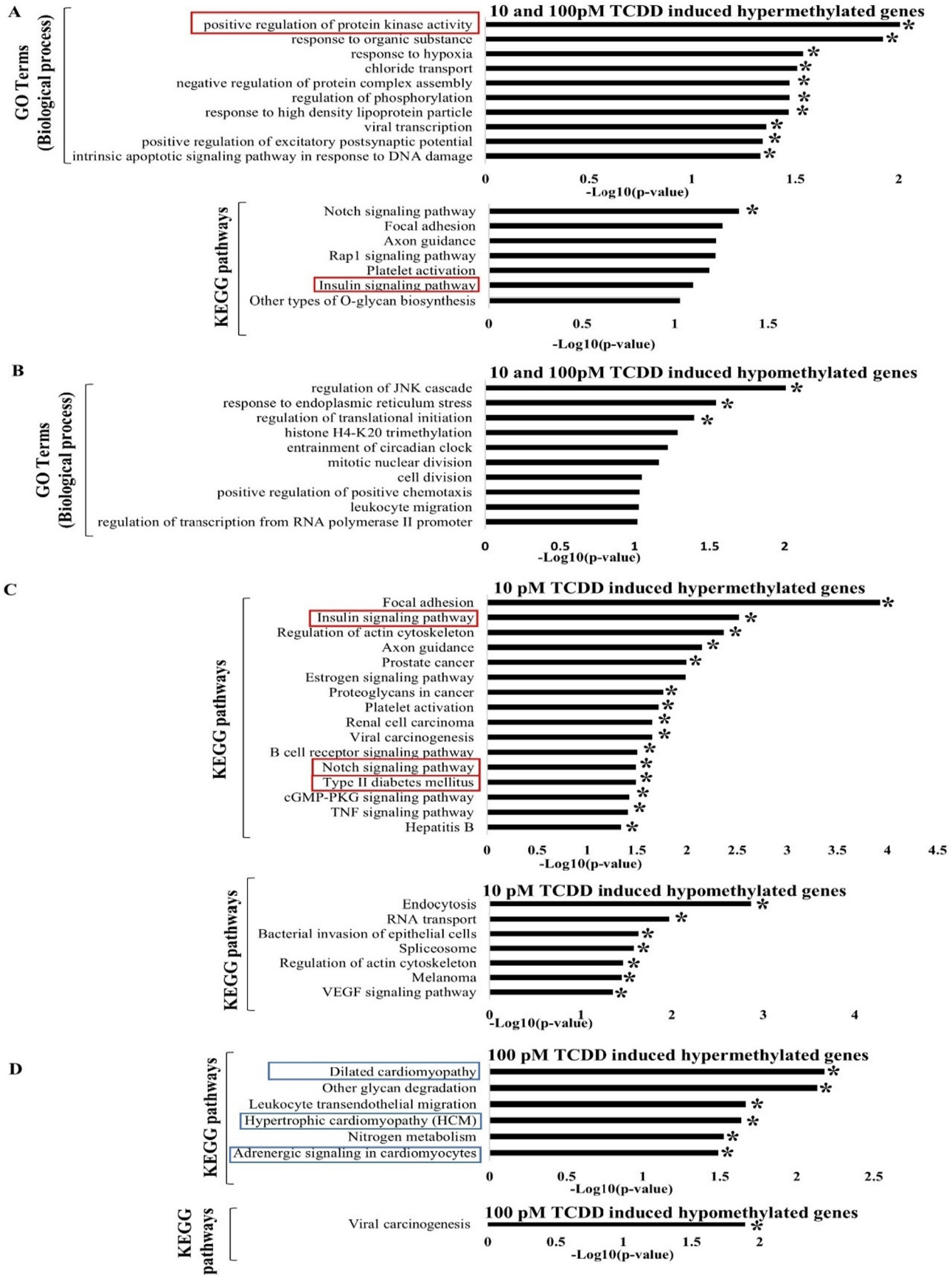

Fig. 4. Gene Ontology and KEGG pathway analysis of differentially methylated genes induced by low doses of TCDD treatments. Top ten GO terms and KEGG pathways enriched in both 10 pM and 100 pM TCDD induced (A) hypermethylated and (B) hypomethylated genes. KEGG pathways enriched in (C) 10 pM or (D) 100 pM TCDD induced hyper- and hypomethylated genes. The enriched GO terms or KEGG pathways were plotted against the −Log10 (P-value). *: significantly enriched, $P < 0.05$.

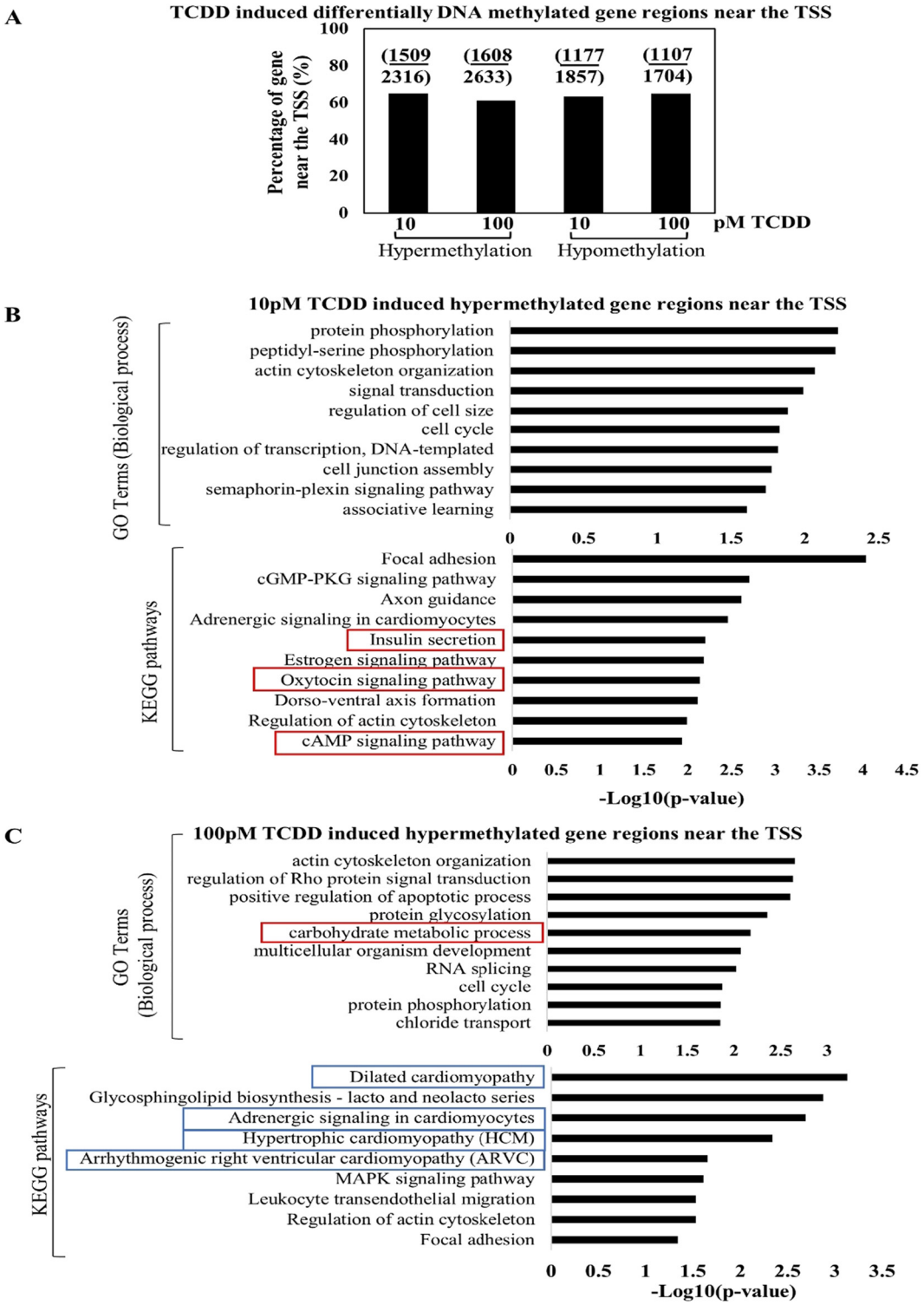

Fig. 5. Gene Ontology and KEGG pathway analysis of TCDD induced differentially methylated gene regions near the TSS. Distribution of TCDD induced differentially methylated genes near the TSS in the (A) undifferentiated hESCs state. Top list of GO terms and KEGG pathways significantly enriched in (B) 10 pM and (C) 100 pM TCDD induced hypermethylated gene regions near the TSS. The enriched GO terms or KEGG pathways were plotted against the −Log10 (P-value).

Fig. 8E).

4. Discussion

The current results demonstrated that TCDD treatment reduced the efficiency of hESCs to early pancreatic lineage differentiation potentials by significantly suppressing *OCT4*, *SOX17* and *PDX1* at DE and PP stages, respectively. The TCDD-induced DNA methylation on PRKAG1, one of the regulators of AMPK pathway, might link to the induced glucose stimulated insulin secretion (GSIS) through the activation of mTOR pathway.

Dioxins such as TCDD were classified as the EDCs with the highest potency of biological activities at picomolar (pM) levels. TCDD was reported to possess dose-dependent effects in different context

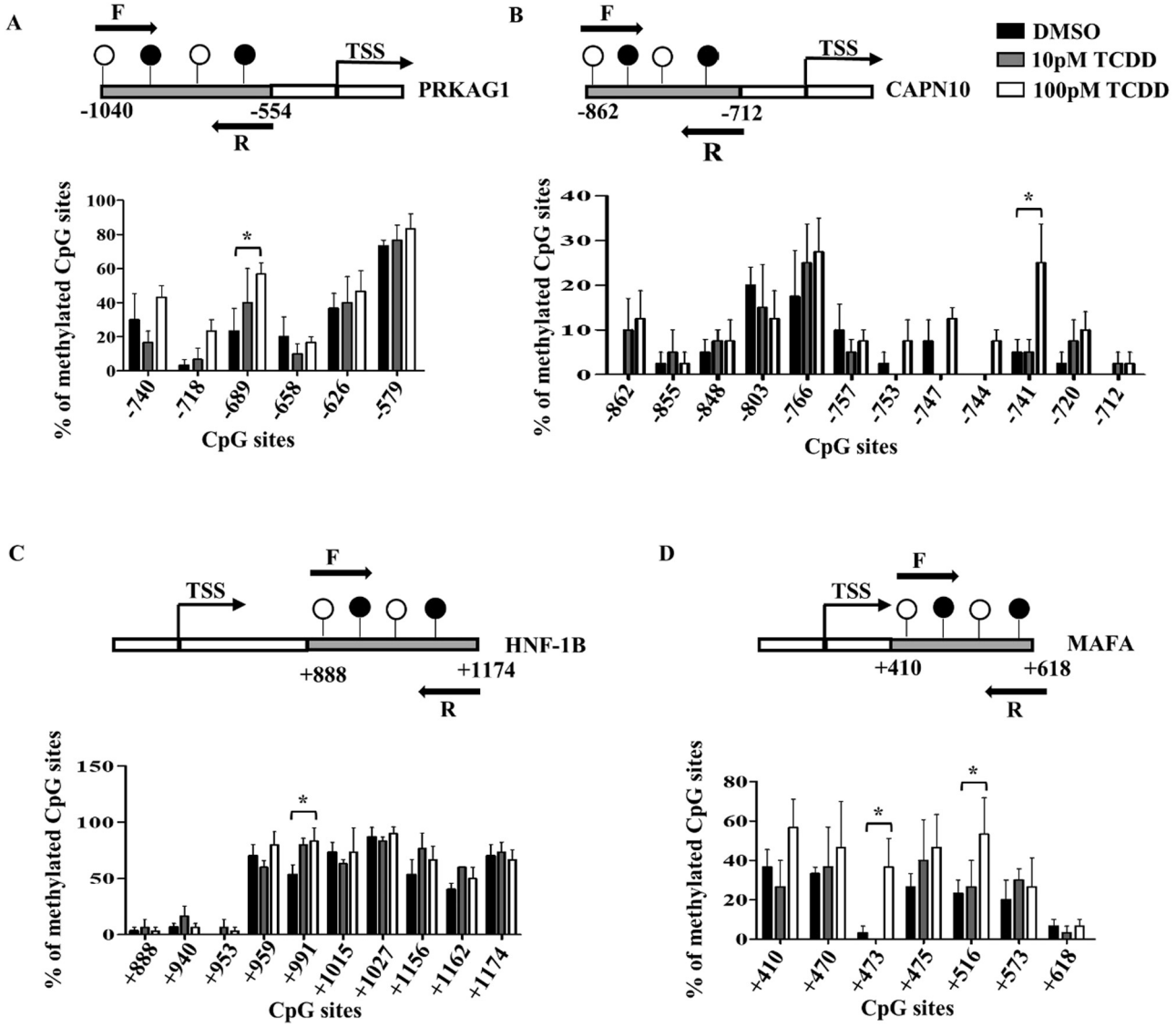

Fig. 6. Validation of the DNA hypermethylation in TCDD treated hESCs. The percentages of methylated CpG sites within the targeted regions (grey) of (A) *PRKAG1*, (B) *CAPN10*, (C) *HNF-1B*, and (D) *MAFA* in hESCs treated with DMSO (black bars), 10 pM (grey bars) and 100 pM (white bars) TCDD by bisulfite sequencing using corresponding forward (F) and reverse (R) primers. All treatment groups were compared with the DMSO control. *: $P < 0.05$; chi-square test; n = 3.

(Santostefano et al., 1999; Gregoraszczuk et al., 2000). Chronic TCDD exposure was associated with endocrine function impairment leading to T2D development in humans (Pesatori et al., 2003; De Tata, 2014). Based on the human TCDD tolerable daily intake (TDI) (10 pg/kg body weight) level (Otarola et al., 2018) and association of TCDD exposure to pancreatic endocrine malfunction, the current study aimed to assess the effects of TCDD at doses similar to human exposure (10 pM and 100 pM) on hESCs differentiation potentials towards pancreatic lineage. Our results showed that both doses of TCDD treatment significantly reduced *OCT4* but not *NANOG* expression in the hESCs and mESCs. It was reported that *OCT4* knockdown in hESCs resulted in robust differentiation towards trophectoderm and mesodermal cell lineage (Zafarana et al., 2009). It is equally important to note that the TCDD induced *OCT4* reduction in the hESCs and mESCs might affect the direction of the ESCs differentiation potentials.

The current data showed that 10 pM and 100 pM TCDD treatment significantly suppressed *SOX17* in the TCDD-treated hESCs and mESCs-derived DE cells. Though not statistically significant, *FOXA2* expression was also reduced at the TCDD treated hESCs-derived DE, FG and PP. It was reported that administration of a single high dose (10 μg/kg) of TCDD at gestational day 15 significantly suppressed *Foxa2* expression in the mouse uterine glands (Burns et al., 2013). Our data showed that 10 pM TCDD treatment significantly repressed *Foxa2* mRNA levels in the mESCs-derived DE. The reduction of *SOX17* or *FOXA2* in the differentiated cells might be due to the altered *OCT4* expressions in the TCDD-treated ESCs. The presence of *OCT4* is pre-requisite for proper *SOX17* and *FOXA2* expression (Ying et al., 2015). Hence, *OCT4* reduction might have impaired DE differentiation.

It was reported that the distal promoter and enhancer regions of *PDX1* were hypermethylated leading to reduced *PDX1* expressions in the pancreatic islets isolated from T2D patients (Yang et al., 2012). Consistently, we observed significantly suppressed *PDX1* expression in the 10 pM TCDD-treated hESCs-derived PP cells, which might be attributed to the inefficient pancreatic lineage differentiation. *FOXA2* is one of the key regulators of *PDX1* during pancreatic lineage cells development (Gao et al., 2008). The reduction of *FOXA2* and *PDX1* at the TCDD-treated hESCs-derived PP stage might also be due to direct effects of TCDD treatments. Although *PDX1* was not hypermethylated in the current methylome data, the fact that *PDX1* expression was regulated by both DNA methylation and histone acetylation (Yang et al., 2012) suggested the involvement of multiple epigenetic regulation.

HDAC7, one of the common genes hypomethylated in the 10 pM and

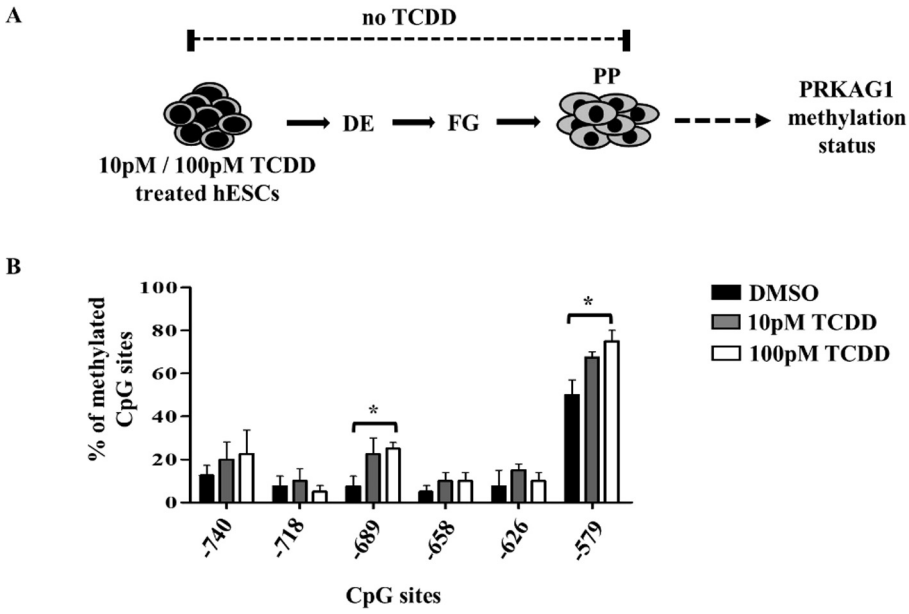

Fig. 7. Maintenance of DNA methylation marks of *PRKAG1* after PP differentiation of TCDD-treated hESCs. (A) Schematic diagram showing the differentiation of DMSO- or TCDD-treated hESCs to DE, FG and PP. The extracted DNA from the PP samples was subjected to DNA bisulfite sequence for analyzing the *PRKAG1* methylation status. (B) DNA methylation pattern of *PRKAG1* in PP cells differentiated from DMSO (black bars), 10 pM (grey bars) or 100 pM (white bars) TCDD treated VAL3 cells. The percentage of methylated CpG sites from −740 to −579 were shown. *: $P < 0.05$; chi-square test; n = 4.

the 100 pM TCDD-treated hESCs, is highly expressed in pancreatic islets from T2D patients and its overexpression significantly decreases insulin content and GSIS in the rat islets (Daneshpajooh et al., 2017). These data suggested that the perturbed methylation status of *HDAC7* might also contribute to the later malfunctions of β-cell in T2D. It is worth to further investigate whether early embryonic TCDD exposure induced HDAC7 hypomethylation could affect pancreatic lineage differentiation potentials and increase the risk of T2D development later in life.

Our group previously reported methylome of 10 pM TCDD treated hESCs. Gene ontology analysis showed that differentially methylated genes were involved in fetal heart, liver functions and response to hypoxia (Lai et al., 2018). However, methyl-CpG binding domain (MBD) protein-enriched genome sequencing used in previous study depended critically on the antibody-based enrichment. This study therefore employed RRBS which had higher sensitivity and extended the study to different low TCDD doses (10 pM and 100 pM). The methylome data obtained here showed that both low and high doses of TCDD treatments induced global DNA methylation changes in hESCs. We matched the differentially methylated genes reported in the pancreatic islets of T2D patients (Dayeh et al., 2014; Volkmar et al., 2012) with the current methylome data induced by the low doses of TCDD treatments. Our findings indicated that about 120 hypomethylated genes induced by the low doses of TCDD were also found to be hypomethylated in the islets of T2D patients.

Analysis of the genes hypermethylated by low doses of TCDD suggested involvement of diverse biological processes and pathways. The current research focused on those related to pancreatic development, functions and pathogenesis. We did not study the differentially methylated genes induced by the 1000 pM TCDD treatment because the implicated pathways and biological processes were not directly related to pancreatic lineage cells development and functions. The TCDD induced hypermethylated genes were significantly enriched in insulin signaling pathway (*PRKAG1*), T2D (*MAFA*), positive regulation of transcription, DNA-templated (*HNF-1B*), cellular response to insulin stimulus (*CAPN10*) (Supplementary Table 3). Calpain-10 (CAPN10) has been widely reported to be a T2D susceptible candidate gene (Ridderstrale and Nilsson, 2008). It was reported that *HNF-1B* suppression might lead to pancreatic beta cell malfunction (El-Khairi and Vallier, 2016) and *MAFA* was found to be significantly reduced in the T2D pancreatic beta cells (Matsuoka et al., 2015). The current data suggest that TCDD might exert diabetogenic effects and early TCDD exposure during embryonic development could increase the risks of T2D development.

PRKAG1 is a less studied AMPK family members. The AMPK family members modulate cellular energy levels to maintain homeostasis of glucose utilization (Jeon, 2016). Although AMPK is known to regulate glucose levels and insulin secretions in pancreatic beta cells (da Silva Xavier et al., 2003), the specific functions of PRKAG1 in pancreatic beta cell physiology and pathology are yet to be comprehensively discovered. TCDD induced hypermethylation of *PRKAG1* might impair key pathways and biological processes significant to pancreatic β-cells physiology. TCDD treated mouse 3T3-L1 adipocytes has altered insulin signaling pathway by silencing IRβ, IRS1, and GLUT4 expressions. The low doses of TCDD induced differential hypermethylated genes in hESCs state might therefore impair pancreatic lineage cells differentiation and beta cell functions via perturbation of insulin signaling pathways. Validation of the selected TCDD induced hypermethylated genes by target base bisulfite sequencing showed that 100 pM TCDD induced hypermethylation near TSS regions of *PRKAG1*, *CAPN10*, *HNF-1B* and *MAFA* in hESCs. Their silence would affect pancreatic lineage cells differentiation leading to functional impairments and pathologic phenotypes (e.g. T2D).

We also studied whether the TCDD-induced epigenetic marks could be maintained during early PP differentiation. We hypothesized that exposure of hESCs to TCDD might cause alterations in the dynamics of epigenetic landscape of some genes that modulate pancreatic β-cell functions. *PRKAG1* was selected for study because it was hypermethylated by both low doses of TCDD treatment. The 100 pM TCDD induced DNA hypermethylation of CpG site located at 689 bp upstream of *PRKAG1* TSS was maintained in the TCDD-treated hESCs-derived PP cells. Similar increasing trend of DNA hypermethylation at the site was also maintained in the 10 pM TCDD treated hESCs-derived PP cells. Another CpG site, 579 bp upstream of TSS was also significantly hypermethylated in the 100 pM TCDD-treated hESCs-derived PP cells, suggested the possible manifestation of TCDD induced subtle effects during pancreatic lineage development. To the best of our knowledge, the current data was the first to demonstrate that TCDD induced differential methylation of *PRKAG1* in the hESCs state could be maintained during PP differentiation. Extrapolation of the finding suggests low doses of TCDD exposure during early embryonic development might introduce epigenetic landmarks in the *PRKAG1* of embryo, which could be maintained throughout pancreatogenesis and alter pancreatic beta cells functions and increase the risk of T2D. Ideally, the gene expression level of PRKAG1 should be measured in the mature β cells

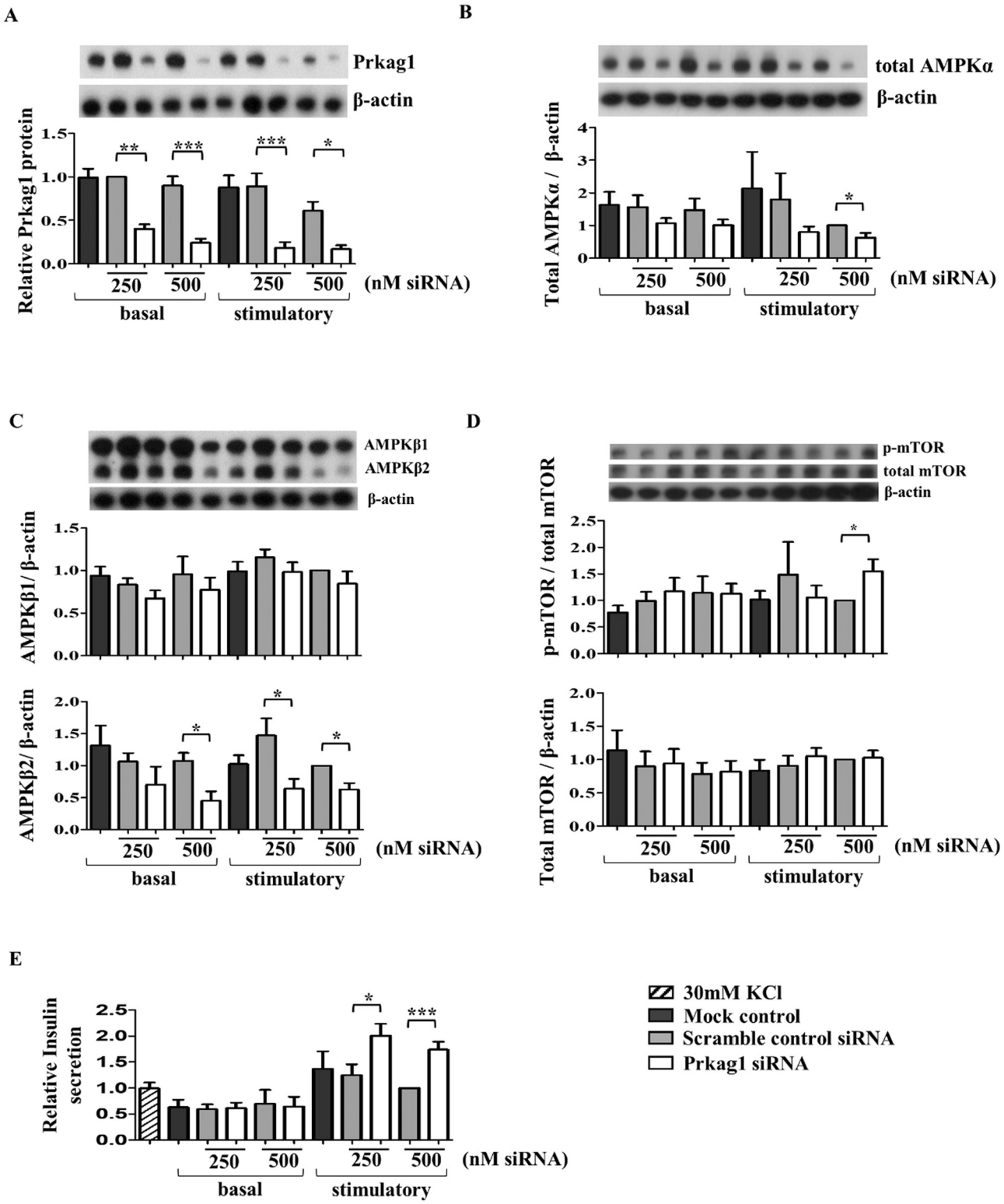

Fig. 8. Effects of Prkag1 knockdown on AMPK, mTOR signaling pathways and GSIS in INS-1E cells. Western blotting analysis of protein levels of (A) Prkag1, (B) AMPKα, (C) AMPKβ1/2, (D) p-mTOR and total mTOR in INS-1E cells and (E) relative insulin secretion in INS-1E conditioned media after transfection of 250 or 500 nM Prkag1 siRNA. The cells were subjected to 30 mM KCl (positive control), 2.5 mM (basal) or 15 mM (stimulatory) glucose treatments for 30 min. Mock transfection or transfection with scrambled siRNA were used as negative controls. Target proteins were normalized with β-actin or total proteins as indicated. *: $P < 0.05$; **: $P < 0.01$, ***: $P < 0.001$; one-way ANOVA and *t*-test; n = 6 for PRKAG1, AMPKα, mTOR, GSIS, n = 4 for AMPKβ1/2.

differentiated from TCDD pre-treated hESC. However, the differentiation of mature insulin producing β-cells from hESC is still challenging in the field. Although pancreatic β cells were differentiated from hESCs, they resembled fetal but not adult β-cells (Hrvatin et al., 2014), which hinder the applicability of the differentiation protocol for the current study. On the other hand, the biological consequence of hypermethylation of PRKAG1 in the cells and/or animals is also technically difficult due to the lack of well-established method of target gene methylation in

cells and/or animals. To understand the effect of alteration of PRKAG1, a less studied member of the AMPK family, on the mature β cells, we performed the knockdown study based on three lines of evidence: 1) hypermethylation proximal to the transcription start site of the promoter regions is correlated with gene suppression (Jones 2012); 2) silencing AMPK activity in MIN6-cells increased insulin secretions (da Silva Xavier et al., 2003); 3) TCDD induced GSIS in INS-1 sells (Kim et al., 2009).

Prkag1 knockdown in INS-1E cells significantly reduced AMPK protein, activated mTOR pathway and elevated GSIS. The result agreed with Kim et al. (2009) showing that GSIS was induced by TCDD treatment in INS-1E cells. Various research groups studied the effects of TCDD exposure on functional β-cell but the research outcomes were still not conclusive. Contrary to the current findings, pancreatic islets isolated from TCDD exposed male mice exhibited reduced GSIS, though no effect was found after 24 h of in vitro exposure of the islets cells to TCDD (Kurita et al., 2009). On the other hand, double knockout of AMPKα1 and 2 in the mouse pancreatic beta cells and brain neurons results in elevated GSIS and blood glucose (Sun et al., 2010). Continuous insulin secretion in pancreatic beta cells induced by secretagogues may result in hyperinsulinemia, insulin resistance, beta cell dysfunction and failure leading to increase beta cell death (Aston-Mourney et al., 2008). The present Prkag1 knockdown induced elevation of GSIS could increase the workload of insulin secretion on the transfected INS-1E beta cells. Over time, the overworking beta cells might be exhausted from continuous Prkag1 knockdown signaling and induced elevation of GSIS leading to defective insulin production, impair insulin secretion and increase in premature beta cell death. AMPK pathway is known to activate Tuberous Sclerosis Complex 2 (TSC2). Pancreatic beta cell specific deletion of TSC2 in mice (beta$TSC2^{-/-}$ mice) activates mTOR and elevated GSIS corresponding to decreased blood glucose levels from 2 to 30 weeks of age followed by significantly reduced GSIS and elevated blood glucose levels from 30 to 50 weeks of age (Shigeyama et al., 2008). mTORC1 and mTORC2 activities were upregulated and downregulated, respectively in the T2D patients and glucose challenged mouse pancreatic islets (Yuan et al., 2017). The current results of Prkag1 knockdown in INS-1E cells mimicked the diabetic condition stated above in that the Prkag1 knockdown also resulted in increased mTORC1 protein content. mTOR1 pathway might be the route involved in the Prkag1 knockdown induced elevated GSIS in the transfected cells.

5. Conclusion

Our results showed that low doses of TCDD induced DNA methylation changes in hESCs and impaired hESCs to early pancreatic lineage cells differentiation potentials. The TCDD-induced hypermethylation of PRKAG1 was maintained in the hESCs-derived PP cells. Prkag1 knockdown in INS-1E cells activated mTORC1 and increased GSIS. Low doses of TCDD exposure during early embryonic development could therefore potentially impair early pancreatic development and functions.

Author contributions

YLL, KFL, WSBY and CKCW conceived and supervised the study. JAK, ACCH, SWF designed and performed the experiments. KPL performed the bioinformatics analysis. JAK, ACCH and YLL wrote the manuscript. All the authors approved the final version of the manuscript.

Funding sources

This work was partly supported by small project funding (grant number: 201409176196) from the University of Hong Kong and Inter-institutional Collaborative Research Scheme (RC-ICRS/17-18/01) from Hong Kong Baptist University.

Declaration of Competing Interest

The authors declare no personal or financial conflicts of interests.

Acknowledgements

We thank the Center for Genomic Science (The University of Hong Kong) for performing reduced representation bisulfite sequence (RRBS) on the TCDD treated hESCs DNA samples. We also thank the Centro de Investigación Príncipe Felipe (CIPF) in Valencia, Spain, who generously donated the hESCs lines VAL3 karyotyped for our study. Finally, we thank Department of Biochemistry, The University of Hong Kong, for providing INS-1E cells and mESCs line (L4) for our experiments.

Appendix A. Supplementary data

Supplementary data to this article can be found online at https://doi.org/10.1016/j.envint.2019.05.079.

References

Alonso-Magdalena, P., Quesada, I., Nadal, A., 2011. Endocrine disruptors in the etiology of type 2 diabetes mellitus. Nat. Rev. Endocrinol. 7, 346–353.
American Diabetes, Association, 2014. Diagnosis and classification of diabetes mellitus. Diabetes Care 37 (Suppl. 1), S81–S90.
Aston-Mourney, K., Proietto, J., Morahan, G., Andrikopoulos, S., 2008. Too much of a good thing: why it is bad to stimulate the beta cell to secrete insulin. Diabetologia 51, 540–545.
Borowiak, M., Maehr, R., Chen, S., Chen, A.E., Tang, W., Fox, J.L., Schreiber, S.L., Melton, D.A., 2009. Small molecules efficiently direct endodermal differentiation of mouse and human embryonic stem cells. Cell Stem Cell 4, 348–358.
Burns, K.A., Zorrilla, L.M., Hamilton, K.J., Reed, C.E., Birnbaum, L.S., Korach, K.S., 2013. A single gestational exposure to 2,3,7,8-tetrachlorodibenzo-p-dioxin disrupts the adult uterine response to estradiol in mice. Toxicol. Sci. 136, 514–526.
Chen, A.C.H., Lee, Y.L., Fong, S.W., Wong, C.C.Y., Ng, E.H.Y., Yeung, W.S.B., 2017. Hyperglycemia impedes definitive endoderm differentiation of human embryonic stem cells by modulating histone methylation patterns. Cell Tissue Res. 368, 563–578.
Consonni, D., Sindaco, R., Bertazzi, P.A., 2012. Blood levels of dioxins, furans, dioxin-like PCBs, and TEQs in general populations: a review, 1989–2010. Environ. Int. 44, 151–162.
Cranmer, M., Louie, S., Kennedy, R.H., Kern, P.A., Fonseca, V.A., 2000. Exposure to 2,3,7,8-tetrachlorodibenzo-p-dioxin (TCDD) is associated with hyperinsulinemia and insulin resistance. Toxicol. Sci. 56, 431–436.
da Silva Xavier, G., Leclerc, I., Varadi, A., Tsuboi, T., Moule, S.K., Rutter, G.A., 2003. Role for AMP-activated protein kinase in glucose-stimulated insulin secretion and preproinsulin gene expression. Biochem. J. 371, 761–774.
Daneshpajooh, M., Bacos, K., Bysani, M., Bagge, A., Ottosson Laakso, E., Vikman, P., Eliasson, L., Mulder, H., Ling, C., 2017. HDAC7 is overexpressed in human diabetic islets and impairs insulin secretion in rat islets and clonal beta cells. Diabetologia 60, 116–125.
Dayeh, T., and C. Ling. 2015. 'Does epigenetic dysregulation of pancreatic islets contribute to impaired insulin secretion and type 2 diabetes?', Biochem. Cell Biol., 93: 511–21.
Dayeh, T.A., Olsson, A.H., Volkov, P., Almgren, P., Ronn, T., Ling, C., 2013. Identification of CpG-SNPs associated with type 2 diabetes and differential DNA methylation in human pancreatic islets. Diabetologia 56, 1036–1046.
Dayeh, T., Volkov, P., Salo, S., Hall, E., Nilsson, E., Olsson, A.H., Kirkpatrick, C.L., Wollheim, C.B., Eliasson, L., Ronn, T., Bacos, K., Ling, C., 2014. Genome-wide DNA methylation analysis of human pancreatic islets from type 2 diabetic and non-diabetic donors identifies candidate genes that influence insulin secretion. PLoS Genet. 10, e1004160.
De Tata, V., 2014. Association of dioxin and other persistent organic pollutants (POPs) with diabetes: epidemiological evidence and new mechanisms of beta cell dysfunction. Int. J. Mol. Sci. 15, 7787–7811.
Diamanti-Kandarakis, E., Bourguignon, J.P., Giudice, L.C., Hauser, R., Prins, G.S., Soto, A.M., Zoeller, R.T., Gore, A.C., 2009. Endocrine-disrupting chemicals: an Endocrine Society scientific statement. Endocr. Rev. 30, 293–342.
El-Khairi, R., Vallier, L., 2016. The role of hepatocyte nuclear factor 1beta in disease and development. Diabetes Obes. Metab. 18 Suppl 1, 23–32.
Eskenazi, B., Mocarelli, P., Warner, M., Needham, L., Patterson Jr., D.G., Samuels, S., Turner, W., Gerthoux, P.M., Brambilla, P., 2004. Relationship of serum TCDD concentrations and age at exposure of female residents of Seveso, Italy. Environ. Health Perspect. 112, 22–27.
Fu, H., Wang, L., Wang, J., Bennett, B.D., Li, J.L., Zhao, B., Hu, G., 2019. Dioxin and AHR impairs mesoderm gene expression and cardiac differentiation in human embryonic stem cells. Sci. Total Environ. 651, 1038–1046.

Gao, N., LeLay, J., Vatamaniuk, M.Z., Rieck, S., Friedman, J.R., Kaestner, K.H., 2008. Dynamic regulation of Pdx1 enhancers by Foxa1 and Foxa2 is essential for pancreas development. Genes Dev. 22, 3435–3448.
Gregoraszczuk, E.L., Wojtowicz, A.K., Zabielny, E., Grochowalski, A., 2000. Dose-and-time dependent effect of 2,3,7,8-tetrachlorodibenzo-P-dioxin (TCDD) on progesterone secretion by porcine luteal cells cultured in vitro. J. Physiol. Pharmacol. 51, 127–135.
Hrvatin, S., O'Donnell, C.W., Deng, F., Millman, J.R., Pagliuca, F.W., DiIorio, P., Rezania, A., Gifford, D.K., Melton, D.A., 2014. Differentiated human stem cells resemble fetal, not adult, beta cells. Proc. Natl. Acad. Sci. U. S. A. 111, 3038–3043.
Huang da, W., Sherman, B.T., Lempicki, R.A., 2009. Systematic and integrative analysis of large gene lists using DAVID bioinformatics resources. Nat. Protoc. 4, 44–57.
IARC, 2012. Chemical Agents and Related Occupations: IARC Monographs on the Evaluation of Carcinogenic Risks to Humans. vol. 100F. pp. 341.
Jeon, S.M., 2016. Regulation and function of AMPK in physiology and diseases. Exp. Mol. Med. 48, e245.
Jones, P.A., 2012. Functions of DNA methylation: islands, start sites, gene bodies and beyond. Nat. Rev. Genet. 13, 484–492.
Kern, P.A., Said, S., Jackson Jr., W.G., Michalek, J.E., 2004. Insulin sensitivity following agent orange exposure in Vietnam veterans with high blood levels of 2,3,7,8-tetrachlorodibenzo-p-dioxin. J. Clin. Endocrinol. Metab. 89, 4665–4672.
Kim, Y.H., Shim, Y.J., Shin, Y.J., Sul, D., Lee, E., Min, B.H., 2009. 2,3,7,8-Tetrachlorodibenzo-p-dioxin (TCDD) induces calcium influx through T-type calcium channel and enhances lysosomal exocytosis and insulin secretion in INS-1 cells. Int. J. Toxicol. 28, 151–161.
Kurita, H., Yoshioka, W., Nishimura, N., Kubota, N., Kadowaki, T., Tohyama, C., 2009. Aryl hydrocarbon receptor-mediated effects of 2,3,7,8-tetrachlorodibenzo-p-dioxin on glucose-stimulated insulin secretion in mice. J. Appl. Toxicol. 29, 689–694.
Lai, K.P., Li, J.W., Chan, T.F., Chen, A., Lee, C.Y.L., Yeung, W.S.B., Wong, C.K.C., 2018. Transcriptomic and methylomic analysis reveal the toxicological effect of 2,3,7,8-tetrachlorodibenzodioxin on human embryonic stem cell. Chemosphere 206, 663–673.
Lee, D.H., Porta, M., Jacobs Jr., D.R., Vandenberg, L.N., 2014. Chlorinated persistent organic pollutants, obesity, and type 2 diabetes. Endocr. Rev. 35, 557–601.
Marshall, C., Hitman, G.A., Partridge, C.J., Clark, A., Ma, H., Shearer, T.R., Turner, M.D., 2005. Evidence that an isoform of calpain-10 is a regulator of exocytosis in pancreatic beta-cells. Mol. Endocrinol. 19, 213–224.
Matsuoka, T.A., Kaneto, H., Kawashima, S., Miyatsuka, T., Tochino, Y., Yoshikawa, A., Imagawa, A., Miyazaki, J., Gannon, M., Stein, R., Shimomura, I., 2015. Preserving Mafa expression in diabetic islet beta-cells improves glycemic control in vivo. J. Biol. Chem. 290, 7647–7657.
Mfopou, J.K., Chen, B., Sui, L., Sermon, K., Bouwens, L., 2010. Recent advances and prospects in the differentiation of pancreatic cells from human embryonic stem cells. Diabetes 59, 2094–2101.
Murea, M., Ma, L., Freedman, B.I., 2012. Genetic and environmental factors associated with type 2 diabetes and diabetic vascular complications. Rev. Diabet. Stud. 9, 6–22.
Neri, T., Merico, V., Fiordaliso, F., Salio, M., Rebuzzini, P., Sacchi, L., Bellazzi, R., Redi, C.A., Zuccotti, M., Garagna, S., 2011. The differentiation of cardiomyocytes from mouse embryonic stem cells is altered by dioxin. Toxicol. Lett. 202, 226–236.
Newbold, R.R., 2011. Developmental exposure to endocrine-disrupting chemicals programs for reproductive tract alterations and obesity later in life. Am. J. Clin. Nutr. 94, 1939S–1942S.
Ngwa, E.N., Kengne, A.P., Tiedeu-Atogho, B., Mofo-Mato, E.P., Sobngwi, E., 2015. Persistent organic pollutants as risk factors for type 2 diabetes. Diabetol. Metab. Syndr. 7, 41.
Otarola, G., Castillo, H., Marcellini, S., 2018. Aryl hydrocarbon receptor-based bioassays for dioxin detection: thinking outside the box. J. Appl. Toxicol. 38, 437–449.
Pesatori, A.C., Consonni, D., Bachetti, S., Zocchetti, C., Bonzini, M., Baccarelli, A., Bertazzi, P.A., 2003. Short- and long-term morbidity and mortality in the population exposed to dioxin after the “Seveso accident”. Ind. Health 41, 127–138.
Ridderstrale, M., Nilsson, E., 2008. Type 2 diabetes candidate gene CAPN10: first, but not last. Curr. Hypertens. Rep. 10, 19–24.
Santostefano, M.J., Richardson, V.M., Walker, N.J., Blanton, J., Lindros, K.O., Lucier, G.W., Alcasey, S.K., Birnbaum, L.S., 1999. Dose-dependent localization of TCDD in isolated centrilobular and periportal hepatocytes. Toxicol. Sci. 52, 9–19.
Schug, T.T., Janesick, A., Blumberg, B., Heindel, J.J., 2011. Endocrine disrupting chemicals and disease susceptibility. J. Steroid Biochem. Mol. Biol. 127, 204–215.
Shigeyama, Y., Kobayashi, T., Kido, Y., Hashimoto, N., Asahara, S., Matsuda, T., Takeda, A., Inoue, T., Shibutani, Y., Koyanagi, M., Uchida, T., Inoue, M., Hino, O., Kasuga, M., Noda, T., 2008. Biphasic response of pancreatic beta-cell mass to ablation of tuberous sclerosis complex 2 in mice. Mol. Cell. Biol. 28, 2971–2979.
Sun, G., Tarasov, A.I., McGinty, J., McDonald, A., da Silva Xavier, G., Gorman, T., Marley, A., French, P.M., Parker, H., Gribble, F., Reimann, F., Prendiville, O., Carzaniga, R., Viollet, B., Leclerc, I., Rutter, G.A., 2010. Ablation of AMP-activated protein kinase alpha1 and alpha2 from mouse pancreatic beta cells and RIP2.Cre neurons suppresses insulin release in vivo. Diabetologia 53, 924–936.
Sun, D., Xi, Y., Rodriguez, B., Park, H.J., Tong, P., Meong, M., Goodell, M.A., Li, W., 2014. MOABS: model based analysis of bisulfite sequencing data. Genome Biol. 15, R38.
Tang-Peronard, J.L., Heitmann, B.L., Andersen, H.R., Steuerwald, U., Grandjean, P., Weihe, P., Jensen, T.K., 2014. Association between prenatal polychlorinated biphenyl exposure and obesity development at ages 5 and 7 y: a prospective cohort study of 656 children from the Faroe Islands. Am. J. Clin. Nutr. 99, 5–13.
Tasnim, D., 2016. The Human Pancreatic Islet Methylome and Its Role in Type 2 Diabetes. Doctoral Dissertation. Faculty of Medicine. Lund University.
Thomson, J.A., Itskovitz-Eldor, J., Shapiro, S.S., Waknitz, M.A., Swiergiel, J.J., Marshall, V.S., Jones, J.M., 1998. Embryonic stem cell lines derived from human blastocysts. Science 282, 1145–1147.
Valbuena, D., Galan, A., Sanchez, E., Poo, M.E., Gomez, E., Sanchez-Luengo, S., Melguizo, D., Garcia, A., Ruiz, V., Moreno, R., Pellicer, A., Simon, C., 2006. Derivation and characterization of three new Spanish human embryonic stem cell lines (VAL -3 -4 -5) on human feeder and in serum-free conditions. Reprod. BioMed. Online 13, 875–886.
Volkmar, M., Dedeurwaerder, S., Cunha, D.A., Ndlovu, M.N., Defrance, M., Deplus, R., Calonne, E., Volkmar, U., Igoillo-Esteve, M., Naamane, N., Del Guerra, S., Masini, M., Bugliani, M., Marchetti, P., Cnop, M., Eizirik, D.L., Fuks, F., 2012. DNA methylation profiling identifies epigenetic dysregulation in pancreatic islets from type 2 diabetic patients. EMBO J. 31, 1405–1426.
Warner, M., Mocarelli, P., Brambilla, P., Wesselink, A., Samuels, S., Signorini, S., Eskenazi, B., 2013. Diabetes, metabolic syndrome, and obesity in relation to serum dioxin concentrations: the Seveso women's health study. Environ. Health Perspect. 121, 906–911.
Wesselink, A., Warner, M., Samuels, S., Parigi, A., Brambilla, P., Mocarelli, P., Eskenazi, B., 2014. Maternal dioxin exposure and pregnancy outcomes over 30 years of follow-up in Seveso. Environ. Int. 63, 143–148.
Winans, B., Nagari, A., Chae, M., Post, C.M., Ko, C.I., Puga, A., Kraus, W.L., Lawrence, B.P., 2015. Linking the aryl hydrocarbon receptor with altered DNA methylation patterns and developmentally induced aberrant antiviral CD8+ T cell responses. J. Immunol. 194, 4446–4457.
Wu, Q., Ohsako, S., Ishimura, R., Suzuki, J.S., Tohyama, C., 2004. Exposure of mouse preimplantation embryos to 2,3,7,8-tetrachlorodibenzo-p-dioxin (TCDD) alters the methylation status of imprinted genes H19 and Igf2. Biol. Reprod. 70, 1790–1797.
Yan, L., Yang, M., Guo, H., Yang, L., Wu, J., Li, R., Liu, P., Lian, Y., Zheng, X., Yan, J., Huang, J., Li, M., Wu, X., Wen, L., Lao, K., Li, R., Qiao, J., Tang, F., 2013. Single-cell RNA-Seq profiling of human preimplantation embryos and embryonic stem cells. Nat. Struct. Mol. Biol. 20, 1131–1139.
Yang, B.T., Dayeh, T.A., Volkov, P.A., Kirkpatrick, C.L., Malmgren, S., Jing, X., Renstrom, E., Wollheim, C.B., Nitert, M.D., Ling, C., 2012. Increased DNA methylation and decreased expression of PDX-1 in pancreatic islets from patients with type 2 diabetes. Mol. Endocrinol. 26, 1203–1212.
Ying, L., Mills, J.A., French, D.L., Gadue, P., 2015. OCT4 coordinates with WNT signaling to pre-pattern chromatin at the SOX17 locus during human ES cell differentiation into definitive endoderm. Stem Cell Rep. 5, 490–498.
Yuan, T., Rafizadeh, S., Gorrepati, K.D., Lupse, B., Oberholzer, J., Maedler, K., Ardestani, A., 2017. Reciprocal regulation of mTOR complexes in pancreatic islets from humans with type 2 diabetes. Diabetologia 60, 668–678.
Zafarana, G., Avery, S.R., Avery, K., Moore, H.D., Andrews, P.W., 2009. Specific knockdown of OCT4 in human embryonic stem cells by inducible short hairpin RNA interference. Stem Cells 27, 776–782.